# Surface electronic structure of Pb(001), Pb(110), and Pb(111)

Klaus Würde, Albert Mazur, and Johannes Pollmann
*Institut für Theoretische Physik II, Festkörperphysik, Universität Münster, D-48149 Münster, Germany*
(Received 13 September 1993; revised manuscript received 29 November 1993)

We report the results of surface electronic-structure calculations for the three low-index faces of elemental Pb. To our knowledge, these are the first calculations for the Pb(110) and Pb(111) surfaces addressing their electronic structure. The underlying bulk crystal is described by a realistic second-nearest-neighbor empirical tight-binding Hamiltonian which includes $s$ and $p$ orbitals and takes spin-orbit coupling into account. The resulting $6s$- and $6p$-derived bands are entirely decoupled. Our Hamiltonian yields the bulk density of states and the occupied bulk energy bands in excellent agreement with the data from x-ray and angle-resolved ultraviolet photoelectron spectroscopy measurements. The electronic structure of the (001), (110), and (111) surfaces is calculated for semi-infinite systems employing the scattering theoretical method. Our calculations predict a number of occupied as well as empty surface states or resonances in the energy regions of both the $s$- and $p$-band projections. All three surfaces show a pronounced resonance around $-8$ eV and a band of bound surface states near $-2$ eV below $E_F$. There are no surface states in the gap between the occupied $s$ and $p$ bands. For exemplary cases we highlight the origin and nature as well as the spatial localization of characteristic surface features.

## I. INTRODUCTION

Electronic properties of elemental group-IV semiconductors and their surfaces have been studied both experimentally and theoretically in enormously great detail in the past decades. On the contrary, the elemental group-IV metal Pb has attracted much less attention although it is of particular interest for a number of reasons. From photoemission studies of the bulk band structure of Pb,[1,2] it is well known that the $5d$, $6s$, and $6p$ bands are energetically well separated. The Pb crystal allows one, therefore, to study independently the metal $s$, $p$, and $d$ bulk bands on an fcc lattice and the low index surfaces of Pb allow one to address the properties of independent metallic $s$ and $p$ bands at (001), (110), and (111) surfaces of an fcc crystal. This situation is very different from the $3d$ and $4d$ transition metals and their surfaces for which the $d$ bands and the $s$-$p$ bands energetically overlap and show strong hybridization effects and effects due to electronic correlations.[3] Pb seems to be a clear-cut case for simple metallic $s$ or $p$ bands for which correlation effects can be expected to be of minor importance. In addition, spin-orbit coupling is essential for an appropriate description of the energy bands of Pb and its surfaces thus allowing one to address relativistic effects on the bulk and surface band structure. Characteristic gaps, e.g., in the projected bulk band structure are to be expected which originate from the considerable spin-orbit splittings of the bulk bands. Finally, Pb overlayers on Si and Ge surfaces have become the subject of intensive studies in the context of Schottky-barrier formation. So the investigation of electronic properties of Pb surfaces is not only an interesting subject in its own right but it is also of basic importance for an understanding of the properties of Pb overlayers on the surfaces of group-IV semiconductors. Nevertheless, so far the electronic properties of only the Pb(001) surface have been studied theoretically by pseudopotential slab calculations[4,5] and the surface energy and stress of the Pb(110) and Pb(111) surfaces have been investigated by a first-principles supercell calculation.[6]

In this paper, we report on applications of the empirical tight-binding scattering theoretical method to electronic structure calculations of all three low-index faces of Pb. The scattering theoretical method has been applied previously to a number of semiconductor surfaces (see, e.g., Refs. 7–10) and was found to be very useful when a realistic Hamiltonian for the underlying bulk crystal is available. We have reported an application of that method to Al surfaces recently,[11] as well. For the Pb surfaces we predict in this paper a number of surface states and resonances. We hope that our results will stimulate further experimental investigations of Pb surfaces.

The paper is organized as follows: In Sec. II we very briefly compile the basic equations of the scattering theoretic formalism. In Sec. III we present our empirical tight-binding method (ETBM) bulk Hamiltonian and discuss the calculated bulk band structure and density of states (DOS) in direct comparison with x-ray photoelectron spectroscopy (XPS) and angle-resolved ultraviolet photoelectron spectroscopy (ARPES) data. Section IV is devoted to a presentation and discussion of the surface electronic structure of the (001), (110), and (111) surfaces of Pb. A short summary in Sec. V concludes the paper.

## II. SCATTERING THEORETIC FORMALISM

The scattering theoretic method is described in detail in Refs. 8 and 9. Here, we very briefly summarize the basic equations of the theory as it applies to metal surfaces. The starting point of the formalism is an unperturbed perfect bulk solid described by a one-electron Hamiltonian $H^o$. A surface is introduced as a planar perturbation $U$ which destroys the three-dimensional periodicity of the crystal with respect to the surface normal.

 

The Hamiltonian of a surface system is then given as $H=H^o+U$. The corresponding surface Green's function contains full information on the surface electronic structure. It is determined by a Dyson equation

$$G(E)=G^o(E)+G^o(E)UG(E) . \quad (1)$$

To take advantage of the planar symmetry, we represent all quantities in the so-called layer-orbital basis $\{|\alpha m,\mathbf{q}\rangle\}$ where $\alpha$ specifies a Bloch orbital, $m$ denotes a particular layer, and $\mathbf{q}$ is a two-dimensional wave vector. The matrix elements of the bulk Green's function read

$$G^o_{\alpha m,\alpha' m'}(\mathbf{q},E)=\lim_{\varepsilon\to 0^+}\frac{1}{2\gamma}\int_{-\gamma}^{+\gamma}e^{i\pi k(m-m')/\gamma}\times\sum_n\frac{c_n^{\alpha m}(\mathbf{q},k)c_n^{\alpha' m'*}(\mathbf{q},k)}{E+i\varepsilon-E_n(\mathbf{q},k)}dk . \quad (2)$$

The $c_n^{\alpha m}(\mathbf{q},k)$ and $E_n(\mathbf{q},k)$ are the expansion coefficients of the Bloch orbitals and the bulk eigenvalues, respectively. Equation (2) is valid for all three low-index faces of an fcc crystal with both $\gamma$ and $\mathbf{q}$ depending on the surface under consideration.

The matrix elements of the surface Green's function $G$ are easily deduced from (1) and (2). For an ideal surface one obtains

$$G_{\alpha m,\alpha' m'}=G^o_{\alpha m,\alpha' m'}-\sum_{\substack{\alpha_s,m_s\\ \alpha_s',m_s'}}G^o_{\alpha m,\alpha_s m_s}[G^o]^{-1}_{\alpha_s m_s,\alpha_s' m_s'}\times G^o_{\alpha_s' m_s',\alpha' m'} . \quad (3)$$

Wave-vector-, energy-, and orbital-resolved layer densities of states are obtained from the surface Green's function as

$$N_{\alpha m}(\mathbf{q},E)=-\frac{1}{\pi}\mathrm{Im}G_{\alpha m,\alpha m}(\mathbf{q},E) . \quad (4)$$

## III. BULK ELECTRONIC STRUCTURE OF Pb

The calculation of the surface Green's function $G$ from the Dyson equation (3) requires the knowledge of the bulk Green's function $G^o$ in the layer-orbital representation. To evaluate the bulk Green's function according to Eq. (2) we need to know the electronic properties of the underlying bulk crystal. In this paper we employ the ETBM to describe the electronic properties of the bulk crystal. It turns out that a very realistic description of the bulk bands is indeed feasible using a seven-parameter ETBM Hamiltonian.

### A. ETBM Hamiltonian for bulk Pb

Contrary to the elemental group-IV semiconductors C, Si, Ge, and $\alpha$-Sn, elemental Pb crystallizes in the fcc structure. Its ground-state configuration is given by [Xe] $4f^{14}5d^{10}6s^26p^2$. The outermost $d$ electrons lie nearly 10 eV below the $6s$ band (approximately 20 eV below the Fermi energy $E_F$). The valence electronic properties of Pb are, therefore, dominated by the $6s$ and $6p$ bands while the $5d$ levels can be viewed as core levels.[2] The $6s$ and $6p$ bands are clearly separated in energy by an $s$-$p$ gap of roughly 3 eV. These facts can be inferred, e.g., from XPS data of Ley *et al.*[1] and photoemission spectroscopy data of Horn *et al.*[2] To describe the bulk $6s$ and $6p$ bands it is thus sufficient to include one $s$ and three $p$ orbitals for each spin in the basis set. It turned out that for a realistic bulk-band-structure description some second-nearest-neighbor matrix elements need to be retained. The tight-binding parameters are determined such that the resulting band structure optimally reproduces previous theoretical results and experimental data. The tight-binding parameters of our ETBM Hamiltonian are given in Table I. As a predominant result of the fitting procedure we note that $V^1_{sp\sigma}$, $V^2_{sp\sigma}$, and $V^2_{pp\pi}$ can be chosen to be zero without loss of a realistic description of the bulk bands. As far as $V^1_{sp\sigma}$ and $V^2_{sp\sigma}$ are concerned, this is of course due to the fact that the $6s$ and the $6p$ bands are decoupled and separated by the 3-eV-wide $s$-$p$ gap. From the magnitude of the interaction parameters obtained in the fitting procedure (see Table I) it becomes clear that the nearest-neighbor $p$ bonding ($V^1_{pp\sigma}$) mainly determines the dispersion of the $6p$ bands. Relativistic corrections become very important for heavy atoms with large atomic number $Z$. It is well known that the Darwin and mass-velocity terms shift the $6s$ bands almost rigidly with respect to the $6p$ bands. This effect can simply be incorporated by adjusting $E_s^0-E_p^0$ (see Table I) accordingly. The spin-orbit coupling has more subtle effects on the band structure. Therefore, we include spin-orbit coupling explicitly in our description. The spin-orbit Hamiltonian matrix elements are expressed as[12]

$$\langle H^{\mathrm{SO}}\rangle=\lambda_{\mathrm{SO}}\langle\alpha\sigma|\mathbf{L}\cdot\mathbf{S}|\alpha'\sigma'\rangle , \quad (5)$$

where $\alpha,\alpha'$ refer to $p$ orbitals at the same lattice site with spin $\sigma$ and $\sigma'$, respectively. The spin-orbit parameter $\lambda_{\mathrm{SO}}$ is determined by fitting the calculated band structure to the measured splitting of the lowest two $p$ bands at the $W$ point. The value of $\lambda_{\mathrm{SO}}$ obtained from an optimal fit of the bulk bands is given in Table I, as well.

### B. Discussion of the bulk energy bands

We now turn to a discussion of the electronic structure of bulk Pb as it results from our ETBM Hamiltonian. The bulk band structure is shown in Fig. 1 together with experimental data from ARPES measurements.[2,13,14] For further comparison, we have included in the figure the

TABLE I. Parameters of the ETBM Hamiltonian for Pb (in eV) as used in the calculations.

| | |
|---|---|
| $E_s^0-E_p^0$ | 9.127 |
| $V^1_{ss\sigma}$ | −0.285 |
| $V^1_{pp\sigma}$ | 1.134 |
| $V^1_{pp\pi}$ | 0.080 |
| $V^2_{ss\sigma}$ | 0.030 |
| $V^2_{pp\sigma}$ | 0.146 |
| $\lambda_{\mathrm{SO}}$ | 0.665 |

unbroadened DOS, a 0.5-eV Lorentzian-broadened DOS of the occupied states and the XPS spectrum of Ley *et al.*[1]

The band structure consists of two groups of bands that are separated by a band gap of 3.1 eV. The lowest band with a width of 4.6 eV is the 6*s* band. The second group of bands is 6*p* derived and shows strong splittings resulting from spin-orbit coupling. For example, at the $W$ point, the two lowest $p$ bands ($W_6, W_7$) are split by 1.7 eV and at the $\Gamma$ point, the $p$ bands are split by approximately 2.0 eV. This splitting at the $\Gamma$ point is analytically given by $3\lambda_{SO}$. As is obvious from Fig. 1, only the lowest two $p$ bands contribute to the valence spectrum whereas the upper $p$ band is entirely empty. The bandwidth of the occupied $p$ bands below $E_F$ amounts to 3.7 eV. It should be noted at this point that higher conduction bands are not taken into account in our restricted *s*-*p* basis set.

Comparing our results with the ARPES data included in Fig. 1, we obtain, in general, very good agreement. We point out a few specific features explicitly: (1) The energetic position and dispersion of the 6*s* band compares very well with ARPES data of Jézéquel and Pollini.[14] The room-temperature data obtained for this band by Horn *et al.*,[2] in particular at the $L$ and $\Gamma$ points, show considerable deviations from the calculated band and from the low-temperature data of Ref. 14. A precise determination of this band in the measurements reported in Ref. 2 was impeded by strong broadening of the peaks that is partly due to the short mean-free path of the photoelectrons destroying the $E(\mathbf{k})$ information to some extent in high-$Z$ materials.[2] (2) Along the $\Lambda$ and $\Sigma$ lines of the Brillouin zone our calculated lowest $p$ band shows excellent agreement with the measured data. (3) The second occupied $p$ band agrees well with the measured $W_6$ level and describes the measured dispersion[14] around the $K$ point reasonably well. (4) The $W_6$-$W_7$ splitting obtained from de Haas–van Alphen effect measurements by Anderson and Gold[15] is exactly adjusted yielding the used value of $\lambda_{SO}$.

TABLE II. Comparison of calculated electronic eigenvalues (in eV) for Pb with experimental results obtained from ARPES data.

| | This work | Theory[a] | Theory[b] | Expt.[a] | Expt.[c] |
|---|---|---|---|---|---|
| $\Gamma_6^+$ | −11.4 | −11.7 | −11.4 | −10.5 | −11.4 |
| $L_6^+$ | −8.3 | −8.2 | −8.3 | −7.3 | |
| $L_6^-$ | −3.7 | −4.3 | −4.5 | −3.7 | |
| $K_5$ | −7.0 | −7.0 | −6.7 | −7.0 | −6.9 |
| $K_5$ | −2.5 | −2.6 | −2.8 | −2.4 | −2.7 |
| $K_5$ | −0.6 | −1.1 | −1.2 | −1.0 | −1.0 |
| $W_6$ | −7.0 | −6.8 | −7.2 | −7.0 | |
| $W_7$ | −2.2 | −2.2 | | −2.4 | |
| $W_6$ | −0.5 | −0.7 | | −0.8 | |
| $X_6^+$ | −6.8 | −6.8 | −6.7 | | −6.8 |
| $X_6^-$ | −3.5 | −3.4 | −3.6 | | −3.4 |

[a]Reference 2.
[b]Reference 16
[c]Reference 14.

For further comparison, we have listed in Table II band-structure energies at high-symmetry points as resulting from our calculations in comparison with the results of previous calculations[2,16] and of experimental

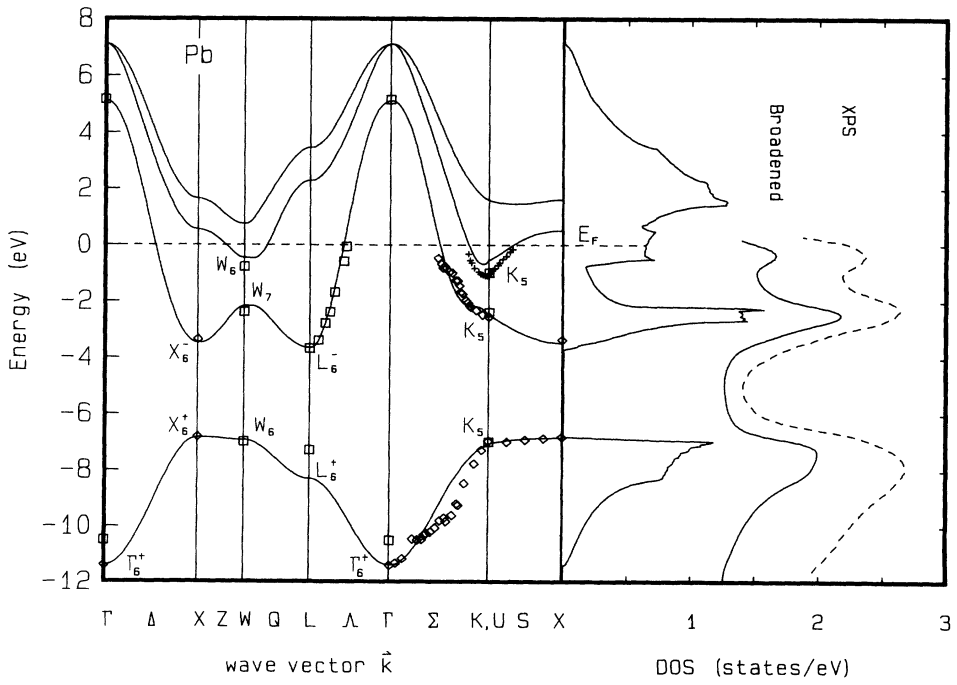


FIG. 1. Bulk band structure and density of states of Pb. The symbols refer to ARPES data given in Refs. 2 and 14, respectively. For comparison we have also shown a 0.5-eV broadened valence-band DOS and the experimental XPS spectrum of Ref. 1 (dashed line).

data.[2,14] Except for the highest occupied $K_5$ energy, we obtain excellent agreement with the well-resolved low-temperature data of Jézéquel and Pollini[14] throughout the occupied bands and very good agreement with the results of previous calculations.[2,16] This very good agreement for the occupied bands is further confirmed in the right panel of Fig. 1 by the very favorable comparison of our broadened DOS of the occupied states with the XPS data of Ley *et al.*[1] Certainly there remain some distinct differences between our tight-binding energies and the local-density approximation (LDA) results of Ref. 2 most noticeably for the $L_6^-$ and $K_5$ states. The latter are close to the Fermi energy and are more properly described in the self-consistent LDA treatment than in an ETBM description.

In summary, we conclude from this section that our ETBM Hamiltonian indeed yields a realistic description of the bulk valence electronic structure of Pb and thus represents a suitable starting point for surface electronic-structure calculations. It should be mentioned that care is needed in the discussion of unoccupied states higher up in the conduction bands due to our restricted basis set.

## IV. SURFACE ELECTRONIC STRUCTURE OF Pb(001), Pb(110), AND Pb(111)

In this section we present and discuss the surface electronic structure of all three low-index surfaces as resulting from our scattering theoretic calculations in the framework of the ETBM. The geometry studied is that of abruptly terminated semi-infinite lattices. The surface band structures are given in Figs. 2 and 3. The projections of the bulk bands along the high-symmetry lines of the respective surface Brillouin zones (SBZ) are shown by the shaded areas. Solid lines denote bound surface states and dashed lines represent pronounced resonances. The irreducible part of each SBZ is shown as an inset.

### A. Pb(001)

Let us first address the Pb(001) surface. The projected bulk band structure (PBS) shows three pronounced gaps and pockets. The gap between $-3.7$ and $-6.8$ eV is the projection of the $s$-$p$ gap in the bulk band structure. In the energy region of the projected $p$ bands there are two pockets. Their extension is significantly influenced by spin-orbit coupling. The lower of these two pockets, for example, closes at the $\bar{M}$ point when spin-orbit coupling is neglected. The width of this pocket at $\bar{M}$ is determined by the $W_6$-$W_7$ splitting of the bulk bands (see Fig. 1 and Table I) induced by spin-orbit interaction. We find five bands ($S_1$–$S_5$) of bound surface states within the $p$-band projections. The band $S_3$ crosses the Fermi level $E_F$.

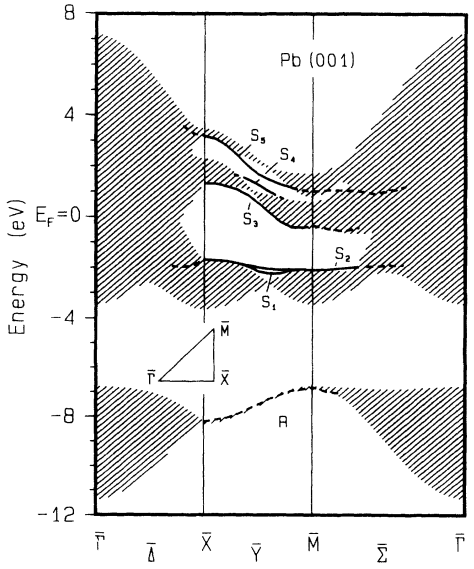


FIG. 2. Projected bulk band structure and surface band structure of ideal Pb(001). The irreducible part of the SBZ is shown as an inset.

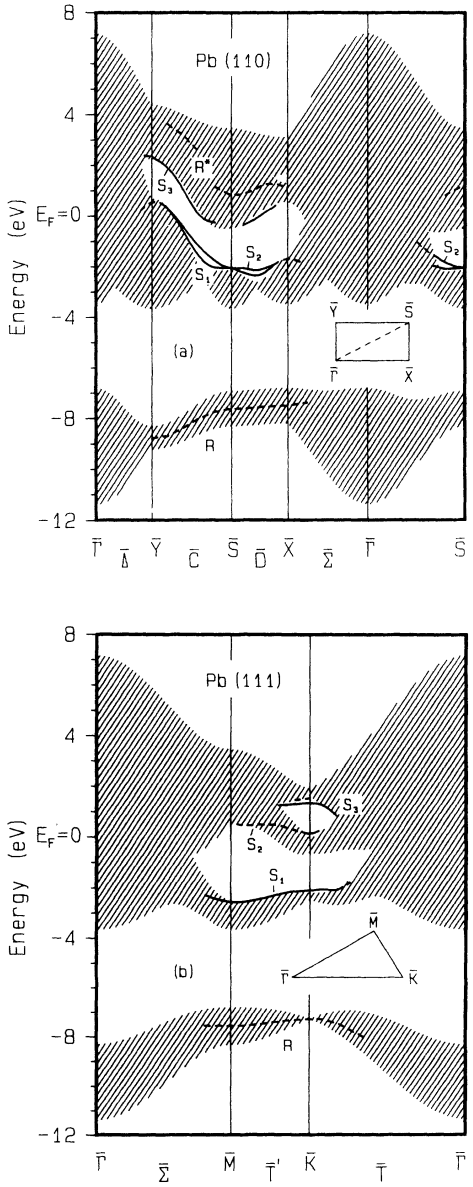


FIG. 3. Projected bulk band structure and surface band structure of the ideal Pb(110) surface (a) and the Pb(111) surface (b). The irreducible parts of the surface Brillouin zones are shown as insets.

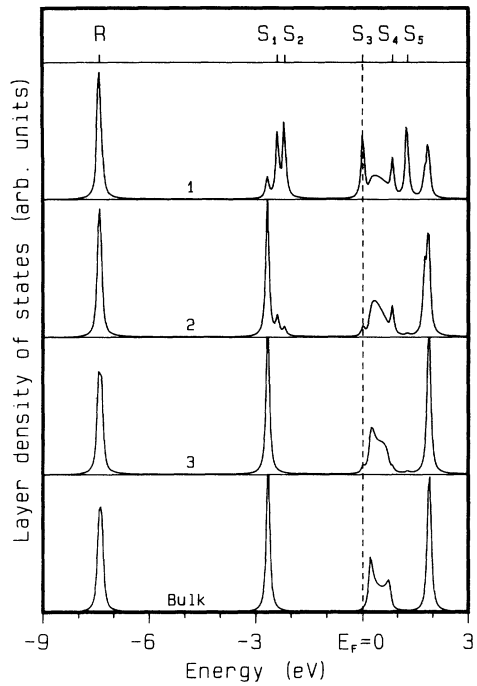


FIG. 4. Layer resolved densities of states at the surface layer (1) and at two subsurface layers (2,3) for a wave vector **q** on the $\bar{Y}$ line. A bulk layer DOS is given for comparison. All densities are broadened by 50 meV.

The occupied bands $S_1$ and $S_2$ show rather weak dispersions and they are located near $-2$ eV below $E_F$. Along the $\bar{Y}$ line these two bands are split by roughly 0.2 eV due to spin-orbit coupling. In addition, we find a rather pronounced resonance band $R$ extending from $\bar{X}$ to $\bar{M}$ in the $s$-band projection.

To highlight the origin, nature, and spatial localization of characteristic surface features, we show in Fig. 4 layer densities of states (LDOS) at that **q** point on the $\bar{Y}$ line of the SBZ at which the $S_3$ band crosses the Fermi level. We see that the bound surface states $S_1$–$S_5$ are all strongly localized near the surface. They mostly reside at the surface layer. The LDOS on the third layer is already very close to the bulk layer DOS. An orbital decomposition of these surface states reveals that the states $S_1$ and $S_2$ are dominated by surface-parallel components (about 90% $p_\parallel$). The state $S_3$ has a significant surface-normal contribution (23% $p_\perp$).

In Fig. 5 we show three-dimensional plots of the LDOS on the first, the second, and a bulk layer along high-symmetry lines from $\bar{\Gamma}$ over $\bar{X}$ and $\bar{M}$ to $\bar{\Gamma}$. The figure clearly reveals that the bulk van Hove singularities are entirely smoothed at the surface. While the 6$s$-band LDOS of the bulk layer between $-6.8$ and $-11.4$ eV at $\bar{\Gamma}$, for example, shows the square-root singularities typical for an $s$ band on an fcc lattice, these singularities are completely smoothed at the surface layer. The same obtains for the superposition of the three $p$ bands higher up in energy. While the bulk LDOS shows pronounced ridges (resulting from van Hove singularities in the bulk DOS) and valleys, the LDOS at the surface is relatively smooth except for the salient features resulting from bound surface states. The LDOS on the second layer is already more similar to the bulk LDOS and confirms that surface effects are mostly restricted to the surface layer. This latter result is observed, as well, in our wave-vector-integrated layer densities of states.

From Figs. 2, 4, and 5, it is obvious that there occur no surface states within the $s$-$p$ gap from $-3.7$ to $-6.8$ eV. This is in agreement with the ARPES data of Horn *et al.*[2] The latter authors questioned the lack of surface states within the $s$-$p$ gap since for a number of 3$d$ and 4$d$ transition metals surface states had been found in an $s$-$p$ gap.[3] As we have pointed out already in the discussion of the bulk bands, Pb is grossly different from the transition metals in that it has well-separated $s$, $p$, and $d$ bands while the latter have $d$ bands that strongly overlap in energy with the $s$-$p$ bands. The occurrence of a surface state in the $s$-$p$ gap of transition-metal surfaces is due to a reduced $s$-$d$ and $p$-$d$ hybridization near the surface. This mechanism is ineffective at Pb surfaces since the 5$d$ states virtually do not interact with the 6$s$ and 6$p$ states. On the contrary, these two separated band groups behave like simple metallic $s$ or $p$ bands on an fcc lattice. When a surface is created, the $s$ or $p$ states, respectively, loose some of their neighbors at the surface and increase their state density near the middle of the respective bands (see Fig. 5 for that matter). In consequence no surface states occur in the $s$-$p$ gap of Pb.

The (001) surface of Pb has been studied previously by Chulkov and co-workers.[4,5] These authors performed a seven-layer-slab pseudopotential calculation including scalar relativistic[4] and fully relativistic[5] corrections. The projected bulk band structure in Ref. 5 and our PBS are in excellent agreement below $E_F$. In agreement with our results Chulkov and co-workers find a pronounced feature in the projected 6$s$ bands between the $\bar{X}$ and $\bar{M}$ point. Their band shows the same dispersion as our resonance $R$ but is slightly higher in energy by 0.1 eV. In addition, the authors of Ref. 5 found a band of surface states centered around $-2.5$ eV near the bottom of the lower pocket. This band is directly related to our $S_1$ and $S_2$ bands which show a small splitting on the $\bar{Y}$ line. Presumably that splitting could not be resolved in the slab calculation of Ref. 5. The states found high above the Fermi level in Ref. 5 show some differences with respect to our results. In particular, Chulkov and co-workers find a pronounced surface state band 6 eV above $E_F$ extending almost throughout the surface Brillouin zone. Our results do not show this band which is, of course, due to our restricted set of eight basis functions (including spin-orbit coupling) while Chulkov and co-workers used hundreds of plane waves and arrived, therefore, at a more complete description of the bands high above $E_F$.

### B. Pb(110) and Pb(111)

Let us now turn to the electronic structure of the (110) and (111) surfaces of Pb which has not been reported previously, to our knowledge. The surface band structures are both shown in Fig. 3 in direct comparison to

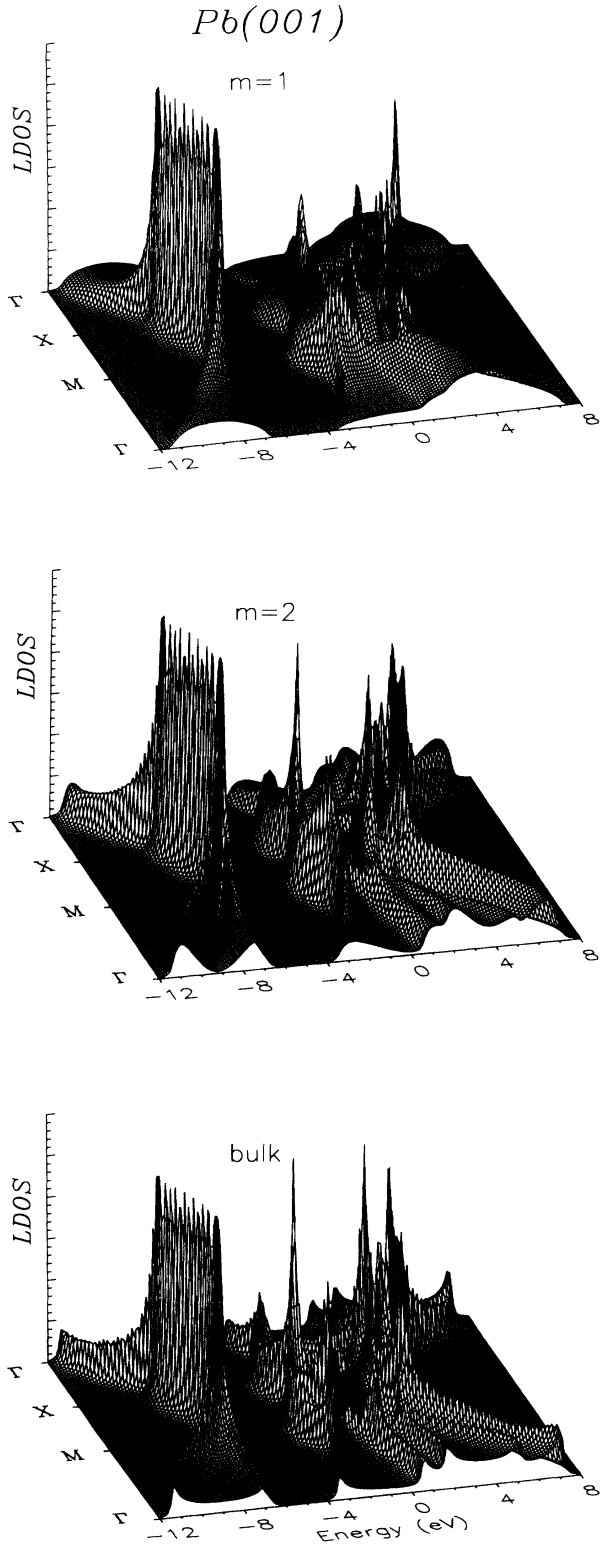


FIG. 5. Layer densities of states on the first, second, and a bulk layer of Pb(001) as a function of energy along the high-symmetry lines of the SBZ. The LDOS is given in arbitrary units and the scales of the three plots are the same.

highlight characteristic similarities and differences in the respective results. Comparing Figs. 3(a) and 3(b) with Fig. 2 we observe that all three projected bulk-band structures are very similar. They are characterized by the projected $s$-$p$ gap and two pockets in the $p$-band projections. The lower of these two pockets is similar for all three surfaces while the higher is most extended at the (001) surface.

For the (110) and the (111) surfaces, as well, we do not obtain surface states in the $s$-$p$ gap, as expected. Both surfaces show a pronounced resonance $R$ within the projected 6$s$ bands very similar to the (001) surface. Again the resonances occur for $\mathbf{q}$ vectors along the edge of the respective surface Brillouin zones and not near the center. Within the $p$-band projections, the (110) and (111) surfaces exhibit three bands of bound surface states $S_1$–$S_3$ which partially become pronounced resonances. At the (110) surface all three of these bands cross the Fermi level. At the (111) surface the $S_1$ band is flat and resides near $-2.2$ eV below $E_F$ while the $S_2$ and $S_3$ bands are above $E_F$. The dispersion of these features is thus much larger at the more open (110) than at the most dense (111) surface. This is a consequence of the fact that at an open-surface directional effects are much more pronounced than at a densely packed surface with a more homogeneous charge density. The bands $S_1$ and $S_2$ as well as $S_3$ at the (110) surface are very similar in origin and nature to the respective states at the (001) surface. In fact, they are highly localized at the surface layer with $S_1$ and $S_2$ having predominantly surface-parallel components (about 70% $p_\parallel$) and $S_3$ again having a significant surface-perpendicular contribution (60% $p_\perp$). The larger perpendicular contribution to $S_3$ at the (110) as compared to the (001) surface is a mere consequence of the openness of the former surface.

Higher up in energy, there is an unoccupied resonance band $R^*$ at the (110) surface that is similar in origin and nature to the band of localized surface states $S_5$ at the (001) surface. Surface-induced features are less pronounced at the (111) surface than at the (001) and (110) surfaces since the number of nearest- and next-nearest neighbors is reduced only to nine and three, respectively, at the former surface. This is clearly to be seen in Fig. 3(b). The resulting states ($S_1$–$S_3$) closely follow the projected band edges and reside near them in energy. The band $S_1$ at the bottom of the larger pocket in the $p$-band projection is not split in contrast to the bands $S_1$ and $S_2$ at the (001) and (110) surfaces, respectively.

### C. Comparison with experiment

As mentioned already in the Introduction, so far, no experimental investigations addressing surface electronic features in particular have been reported. Both Horn *et al.*[2] and Jézéquel and Pollini[14] have taken ARPES data with synchrotron radiation in order to map out the Pb bulk bands along high-symmetry lines of the bulk Brillouin zone. Horn *et al.*[2] used a Pb(111) crystal and Jézéquel and Pollini[14] studied Pb(001) and Pb(110). The authors did not report any surface states for all three surfaces. To identify the signature of Pb surfaces in ARPES

data, it is necessary to take additional off-normal-emission spectra. We hope that our predictions of surface states at all three low-index faces of Pb will stimulate experimental ARPES measurements on these surfaces.

If experimental results on the surface electronic structure of Pb surfaces become available, one will certainly have to consider surface relaxation effects in the theory for the sake of meaningful comparisons. However, we do not expect strong modifications of our results by surface relaxation. To this end, we have carried out a few test calculations for Pb(110) using the experimentally determined surface relaxation geometry and we found only marginal rigid shifts of the surface states $S_1$, $S_2$, and $S_3$. For the convenience of the reader, we summarize in Table III what is known experimentally about multilayer relaxation at the low-index surfaces of Pb. Obviously, the relaxation behavior is dominated in all three cases by a considerable inward relaxation of the top layer and relatively small alternating relaxations [except for Pb(111)] of the following subsurface layers. The most open (110) surface shows the largest relaxation while the most densely packed (111) surface exhibits the smallest relaxation effects. Therefore, we have chosen the (110) surface for the above-mentioned test calculations. In consequence of the homogeneity of the metallic charge density of Pb, as opposed to the group-IV semiconductors, a small surface relaxation is not expected to have significant influence on the surface electronic spectrum.

TABLE III. Experimental data on the relaxation of the first three layers of the low-index surfaces of Pb. Here $\Delta d_{ij}$ is the percent change of the distance between layers $i$ and $j$, as compared to the respective ideal bulk layer distance.

| | Pb(001)[a] | Pb(110)[b] | Pb(110)[c] | Pb(111)[d] |
|---|---|---|---|---|
| $\Delta d_{12}$ | −8.0% | −15.8% | −16.3% | −3.5% |
| $\Delta d_{23}$ | +3.1% | +2.7% | +3.4% | +0.5% |
| $\Delta d_{34}$ | −3.0% | −3.0% | −4.0% | +1.6% |

[a]Reference 17.
[b]Reference 18.
[c]Reference 19.
[d]Reference 20.

## V. CONCLUSIONS

In summary we have reported and discussed in some detail the surface electronic structure of the three low-index faces of Pb. We have shown that the electronic properties of the underlying bulk crystal can very accurately be described by an ETBM Hamiltonian retaining only the most important nearest- and next-nearest-neighbor interaction matrix elements of the 6*s* and 6*p* states without the need of including any *s-p*, *s-d*, or *p-d* hybridization terms. Inclusion of spin-orbit coupling turned out to be mandatory and leads to a calculated bulk band structure which is in excellent agreement with XPS and ARPES data.

The gross features of the surface electronic structure for all three surfaces are found to be largely similar and to show only a weak dependence on the different surface roughness of the three studied surfaces. Spin-orbit coupling enhances the pockets in the projected *p* bands significantly and bands of bound surface states are found in these pockets. Common to all three surfaces is the occurrence of a pronounced resonance within the projected 6*s* bands and of salient bands of localized surface states near −2 eV below $E_F$. At the (001) and (110) surfaces these bands are split by roughly 0.2 eV in small regions of the SBZ. This splitting is a consequence of spin-orbit coupling. We find no surface states in the projected *s-p* gap in complete agreement with all available ARPES data and we have given reasons for the lack of surface states in this gap. In addition, we find empty surface states above $E_F$ at all three surfaces. All surface features occur for wave vectors along the edges of the surface Brillouin zones but not near the zone centers. Thus off-normal emission ARPES and angle-resolved inverse-photoemission-spectroscopy investigations are necessary in order to identify the predicted states experimentally.

## ACKNOWLEDGMENTS

One of us (K.W.) gratefully acknowledges financial support from the Graduiertenförderungs-Programm des Landes Nordrhein-Westfalen during the final stages of this work.

[1]L. Ley, R. Pollak, S. Kowalczyk, and D. A. Shirley, Phys. Lett. **41A**, 429 (1972).
[2]K. Horn, B. Reihl, A. Zartner, D. E. Eastman, K. Hermann, and J. Noffke, Phys. Rev. B **30**, 1711 (1984).
[3]See, e.g., F. J. Himpsel, Adv. Phys. **32**, 1 (1983).
[4]E. V. Chulkov, V. M. Silkin, and I. Yu. Sklyadneva, Surf. Sci. **231**, 9 (1990).
[5]E. V. Chulkov, Yu. M. Koroteev, and V. M. Silkin, Surf. Sci. **247**, 115 (1991).
[6]M. Mansfield and R. J. Needs, Phys. Rev. B **43**, 8829 (1991).
[7]J. Pollmann and S. T. Pantelides, Phys. Rev. B **18**, 5524 (1978).
[8]J. Pollmann, in *Festkörperprobleme (Advances in Solid State Physics)*, edited by J. Treusch (Vieweg, Braunschweig, 1980), Vol. XX, p. 117.
[9]M. Schmeits, A. Mazur, and J. Pollmann, Phys. Rev. B **27**, 5012 (1983).
[10]J. Pollmann, R. Kalla, P. Krüger, A. Mazur, and G. Wolfgarten, Appl. Phys. A **41**, 21 (1986).
[11]K. Würde, A. Mazur, and J. Pollmann, Phys. Status Solidi B **179**, 399 (1993).
[12]D. J. Chadi, Phys. Rev. B **16**, 790 (1977).
[13]G. Jézéquel, A. Barski, P. Steiner, F. Solal, P. Roubin, R. Pinchaux, and Y. Petroff, Phys. Rev. B **30**, 4833 (1984).
[14]G. Jézéquel and I. Pollini, Phys. Rev. B **41**, 1327 (1990).
[15]J. R. Anderson and A. V. Gold, Phys. Rev. **139**, A1459 (1965).
[16]T. L. Loucks, Phys. Rev. Lett. **14**, 1072 (1965).

[17]R. F. Lin, Y. S. Li, F. Jona, and P. M. Marcus, Phys. Rev. B **42**, 1150 (1990).
[18]J. W. M. Frenken, J. F. van der Veen, R. N. Barnett, U. Landman, and C. L. Cleveland, Surf. Sci. **172**, 319 (1986).
[19]Y. S. Li, J. Quinn, F. Jona, and P. M. Marcus, Phys. Rev. B **40**, 8239 (1989).
[20]Y. S. Li, F. Jona, and P. M. Marcus, Phys. Rev. B **43**, 6337 (1991).

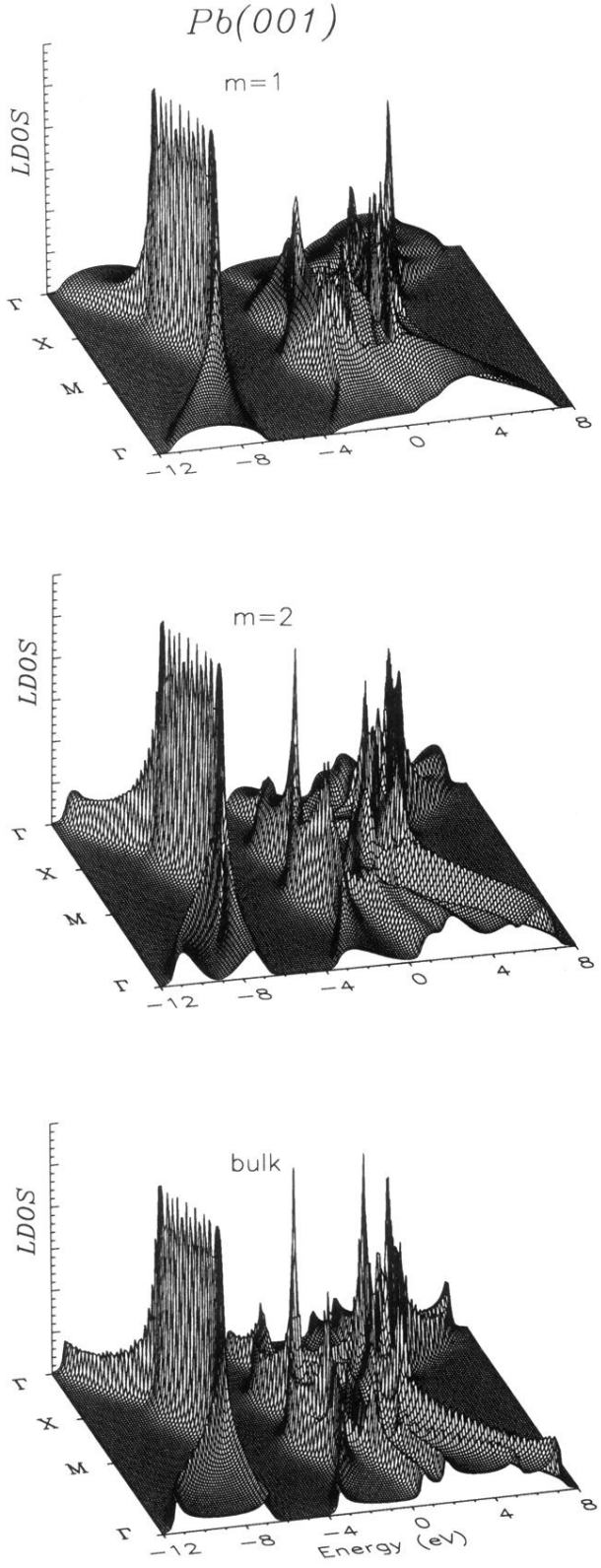


FIG. 5. Layer densities of states on the first, second, and a bulk layer of Pb(001) as a function of energy along the high-symmetry lines of the SBZ. The LDOS is given in arbitrary units and the scales of the three plots are the same.